JPE 16-4-34

http://dx.doi.org/10.6113/JPE.2016.16.4.1612
ISSN(Print): 1598-2092 / ISSN(Online): 2093-4718

Fault Immune Pico-Hydro Powered Base Station of Remote Telecommunication Tower

Vishal Verma†, Peeyush Pant*, and Bhim Singh**

†,*Department of Electrical Engineering, Delhi Technological University, Delhi, India
**Department of Electrical Engineering, Indian Institute of Technology, Delhi, India

Abstract

This paper presents the dynamic excitation control of a siphon-turbine coupled pico-hydro powered cage rotor induction generator and load matching for off-grid electricity generation. Through the proposed dual-role of the current-controlled voltage source converter (VSC), acting as static synchronous compensator and load controller, real and reactive power are dynamically controlled in a decoupled manner with a self supported DC-bus. The proposed scheme entails minimal computation for ensuring the rated (set) capacity of real power. The scheme also exhibits fault immunity for protection, thus enabling the effective handling of constant power electrical loads presented by base telecom station towers in remote locations. The performance of the system is evaluated under MATLAB/Simulink and is experimented through a developed hardware prototype. Simulation and experimental results show close conformity and validate the effectiveness of the proposed scheme.

Key words: Isolated base telecom station, Load controller, Pico-hydro, Siphon turbine, STATCOM

I. INTRODUCTION

The installation of additional telecom- towers is mandatory for remote wireless communication. A typical base telecom station (BTS) tower requires three-phase 50 Hz supply and consumes power in the 2–10 kW range [1]. Remotely located telecom towers conventionally employ three-phase diesel generator sets and hybrid supply systems. However, pollution, costly maintenance, poor efficiency, difficult approach, and high recurring fuel cost are major issues. As sustainable solutions, renewable resources entail low cost and low carbon footprint and have thus emerged as a solution to the energy requirements of remotely located telecom towers [2]. Popular renewable sources, such as solar photovoltaic and wind turbines, fall short because of their intermittency, costly storage, poor efficiency, and high routine maintenance requirements [3].

In small-scale pico hydro generation (PHG), employing a cage rotor induction generator (IG) coupled with a siphon turbine is advocated as a suitable approach [4]. Small capacity IGs exhibit low reactance-to-resistance ratio and low mechanical inertia, and they present a weak source before the load. Moreover, when a weak grid caters to perturbing loads, issues such as voltage sag/swell, harmonics, unregulated frequency, and voltage collapse pose problems for power supply [5]. Investigations reported so far address only a few of the aforementioned issues, namely, the voltage regulation and harmonic compensation of self-excited induction generators (SEIGs) by employing pulse-width modulation (PWM) rectifiers and static synchronous compensator (STATCOM) [6]. Furthermore, the issue of the unregulated frequency of SEIGs amid perturbing loads is addressed by employing electronic load controllers, and investigations are aimed at size reduction and harmonics elimination [7]. However, as a result of the presence of large fixed excitation capacitors, several issues emerge during sudden generator under-loading, load controller malfunction, abnormal fault causing voltage sag/swells, excess winding stress, insulation failure/breakdown, etc., in a weak off-grid power supply. Stabilization issues emerge because BTS towers often experience intermittent operations of fast-acting linear and non-linear constant power loads, such as those of switched mode power supply [1], [2]. Therefore, investigations are due to provide concrete solutions to inherent self-protection and

Manuscript received Aug. 14, 2015; accepted Jan. 26, 2016
Recommended for publication by Associate Editor Jee-Hoon Jung.
†Corresponding Author: vishalverma@dce.ac.in
Tel: +91-11-27871018, Fax: +91-11-27871023, Delhi Tech. University
*Dept. of Electrical Eng., Delhi Technological University, India
**Dept. of Electrical Eng., Indian Institute of Technology, India

good voltage regulation requirements even under perturbing and fast switching loads.

The present study proposes a suitable siphon turbine coupled with an IG to cater to the electricity requirements of remote BTS towers (Fig. 1) with a pico hydro source. The proposed control scheme draws rated power from the IG to make it optimally efficient and easy to operate. Moreover, the variable reactive power for the requisite excitation of generators is dynamically supplied by a current-controlled voltage source converter (VSC) with a tank capacitor at the DC bus and a small fixed capacitor bank for ripple filtering and partly providing excitation for the IG. The VSC regulates generator voltage amid varying reactive power-hungry loads because of VSC acting as a STATCOM in the circuit, whereas, frequency is regulated by load matching by dumping excess energy on the DC bus, which is eventually bleeded through a chopper/bleeder to avoid the duplication of circuits. The control scheme makes the supply system immune to faults without the need for additional costly hardware. It also offers fast self-protection by ceasing VSC pulses against abnormalities, such as over/under-voltages/current, load controller malfunction, and instant load removal; such self-protection is not possible if a self-excitation capacitor sustains the generator. The performance of the system is evaluated in MATLAB/Simulink and experimentally validated on a developed hardware prototype (2.2 kW, 415 V, 50 Hz). The simulation and experimental results show close conformity and validate the effectiveness of the proposed scheme.

II. System Configuration

The proposed system shown in Fig. 2 represents a remote PHG system employing a siphon turbine that acts as a prime mover duly coupled with an IG. The combination of the IG and a small filter capacitor bank at its terminals is henceforth referred to as a pico-hydro generating source (PHGS) connected at the point of common coupling (PCC) with a self-supported VSC. The three-phase VSC is integrated with a load controller on the DC bus to meet the reactive power requirement of PHG and the required load with load matching. The VSC is connected at the PCC by interfacing inductors. The considered loads are intermittent, constant power loads (CPLs) connected in parallel, thus emulating a remote BTS when observed from the PCC. The scheme operates in power decoupling mode to present voltage regulation and load matching at the PCC.

III. Analysis of Constant Power Load

The electrical loads of a typical BTS are often intermittent CPLs before the PCC. The characteristic of a CPL (capacity P_{load}) is depicted in Fig. 3(a), which is analyzed by piecewise

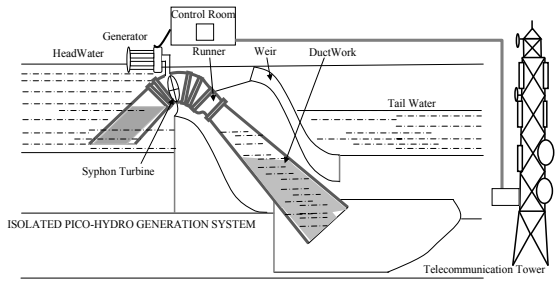

Fig. 1. Schematic diagram of the pico-hydro powered BTS.

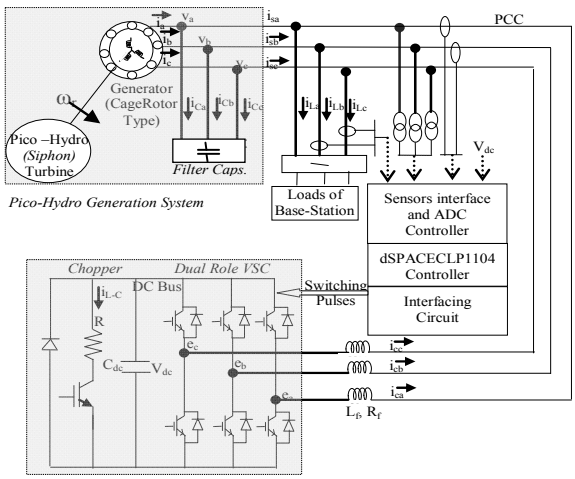

Fig. 2. Schematic diagram of the proposed system.

linearizing the nonlinear supply perturbations of the PCC. Load intermittency in a weak source often causes voltage sag ΔV (say) at the PCC, which results in the displacement of the current ΔI of the current I_1 and thus disturbs the equivalent resistance perceived by the PCC, which is expressed as:

$$R_e = \frac{P_{load}}{(I_1)^2} \quad and \quad R_{e1} = \frac{P_{load}}{(I_1 + \Delta I)^2} \approx \frac{P_{load} / I_1^2}{1 + \frac{2\Delta I}{I_1}} \tag{1}$$

Through Taylor's series expansion and approximation in equivalent resistance, Equ. (1) becomes

$$R_{e1} = R_e - 2.R_e \frac{\Delta I}{I_1} \tag{2}$$

As observed in Equ. (2), the net decline in R_e provokes the escalation of the current drawn by the load that exacerbates the decline in voltage at the PCC. Such loading, when connected at the terminal of the self-excited IG, produces a cascading effect on the PCC voltage (V_{PCC}) and results in voltage collapse. The surface plot depicted in Fig. 3(b) presents the voltage collapse phenomenon observed on the PCC of the weak distribution grid fed by SEIG in terms of the reference currents corresponding real and reactive powers. As observed in Fig. 3(b), under nominal conditions, the operating point lies in the active region "A", where the IG is magnetized by the rated current with a nominal voltage at its terminals. Any voltage drop (ΔV) by load intermittency at the

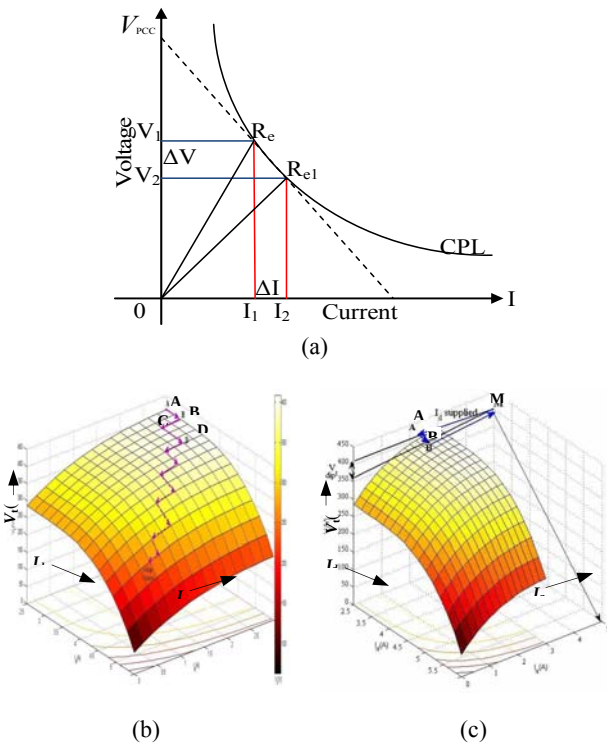

Fig. 3. (a) Dynamic behavior of CPL. (b) Surface plot depicting voltage collapse when IG (excited by fixed capacitors) feeds constant power loads. (c) Surface plot depicting voltage recovery at IG terminals by proposed decoupled control of real and reactive power.

PCC of the SEIG disturbs the operating point from "A" to a new operating point at "B" and reduces the magnetizing current because it depends on voltage and is supplied by fixed capacitors installed at the PCC. The voltage sag (ΔV) causes the under-excitation of the IG, which further deepens the voltage sag at the PCC of the weak distribution grid. The plot in Fig. 3(b) shows that the point of operation follows the voltage diminishing path from B-C-D, which recursively pushes the SEIG out of generation and causes voltage collapse in the weak distribution grid.

The dynamic compensation of real and reactive power through decoupled control by the proposed dual-role self-supported VSC additionally supplies the requisite reactive power that keeps the magnetizing current nearly constant. In this way, a further decline in voltage and the voltage collapse of the IG are prevented, especially when the IG caters to intermittent CPL loads at the PCC. The process of such compensation can be understood through the operation of the VSC in decoupled mode. The decoupled control of real and reactive power facilitates voltage regulation and frequency at the PCC, respectively. The reference can command currents (I_d and I_q) of the VSC. Mathematically, it may be expressed as

$$\Delta V=\xi(\Delta I_q) \quad \text{and} \quad \Delta f=\Upsilon(\Delta I_d) \tag{3}$$

$$\text{and} \quad P_{IG}=P_{load}+P_{LC}+\frac{1}{2}J\omega^2 \tag{4}$$

where P_{IG} is the rated capacity of the IG, P_{load} is the real power drawn by the CPL, P_{LC} is the power dispensed to the load controller, and J is the moment of inertia of the IG.

To regulate source frequency, real power extraction from PHG terminals (P_{IG}) should be maintained at a fixed level. CPL demands real power and causes voltage sag (ΔV) at the PCC. The proposed decoupled control of real and reactive power for voltage and frequency regulation is presented in the surface plot shown in Fig. 3(c). As voltage sag shifts from operating point "A" to operating point "B", the proposed scheme reactive power is dynamically supplied by the current-controlled STATCOM, and the magnetization of the IG is maintained during the voltage sag (refer to Equ. (3)). To compensate for the voltage sag (ΔV), reactive power is dynamically supplied by the STATCOM, which allows the swift recovery of the voltage sag at the PCC and pushes the operating point toward "M" (refer to Fig. 3(c)). Real power is instantly supplied by the fast extraction of kinetic energy from rotor inertia, followed by load matching provided by the load controller action. The intermittent real power demand (ΔP), which is met by trapping stored energy from rotor inertia, trims down the frequency. However, the follow-up action of the load controller steadily matches real power (ΔP), which corresponds to a raised current margin (ΔI), and restricts the margin of real power (ΔP). The load controller current (ΔI) corresponding to the intermittency is given as

$$\Delta I=\frac{\delta V_{dc}}{R} \tag{5}$$

$$\Delta P=\frac{(\delta V_{dc})^2}{R} \tag{6}$$

where δ = duty cycle, V_{dc} = DC bus voltage, and R = load controller resistance. The net effect of dynamic reactive power control and load matching (Equs. (3)–(6)) by the proposed VSC addresses the voltage recovery in weak PHG systems. As depicted in Fig. 3(c), the real power reverts to the operating point of the IG near point "A" (active region for IG operation). Consequently, IG operation remains live even under intermittency amid CPL loads connected at the PCC. The proposed analysis is validated through simulation and experimentation on the developed prototype.

IV. Control Strategy

Fig. 4 shows the schematic diagram of the control scheme employed for the dual-role converter enacting as STATCOM and load controller at the DC bus, to support loads emulating the CPL of the BTS. The proposed control scheme ensures that the VSC supplies the requisite amount of reactive power demanded by the IG and the connected loads at the PCC, in addition to damping real power under light load conditions for power matching. The scheme respects the limits of the presented control to draw the rated current through the IG.

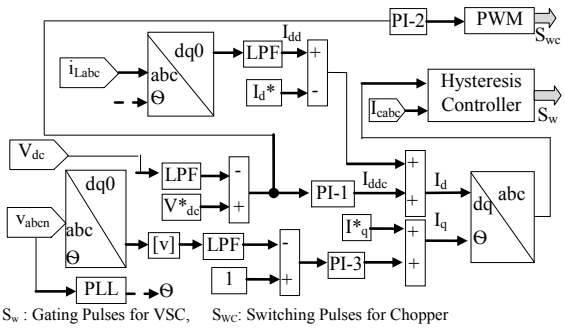

Fig. 4. Proposed control scheme for dual-role VSC.

The load perturbations are maintained via energy transfer across the DC bus. The control relies on the fact that any increase in the DC bus voltage transfers real power to the load controller connected at the DC bus to match the load with the rated value by keeping the DC bus voltage constant. Consequently, the current at the source terminal becomes sinusoidal, along with the regulation of voltage and frequency at its terminals. The current control of the VSC effectively compensates for the perturbations of the real and reactive power demand of the low-capacity IG. The control strategy is realized as follows:

A) DC Bus Control: Computation of VSC current I_d

B) Voltage Regulation: Computation of VSC Current I_q

C) Determination of Synchronization Angle

D) Frequency Control: Load Control Implementation

The control strategy is implemented through three proportional integral (PI) controllers for different components of control. The sensed DC bus voltage is processed through a low-pass filter and compared with a reference DC bus voltage. The error is processed through the PI-1 controller, which estimates the real current (I_{ddc}) component required to maintain the DC bus voltage at the reference value, whereas the deviation of loading from the rated value on the generator simultaneously affects the DC bus voltage because the energy to be transferred across the DC bus plays a vital role. Thus, other components corresponding to the real power components of the load current (I_{dd}) are estimated through Park's transformation of load currents and added to the current determined with the PI controller (PI-1), which is responsible for the voltage regulation of the DC bus and the transfer of power deviation from the rated value of the PHG source. Thus, the sum of the two current components, i.e., I_{ddc} and ΔI_d, provides a net estimation of the reference real current, which in turn maintains the DC bus voltage and operates the PHG source at a rated value by extracting equalizing power from the VSC on the DC bus.

The net estimation of the current corresponding to reactive power I_q, is achieved through the accumulation of fixed reactive currents from the component required by the IG. The current corresponding to reactive power is required for the voltage regulation at the PCC. The estimation of the said component is derived from the per unit rms (root mean square) value of the sensed voltage and is compared with the unit reference voltage to regulate the reactive power through the PI controller (PI-3).

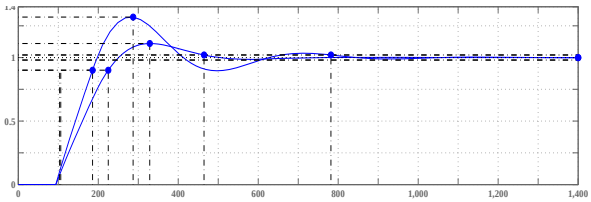

Fig. 5. Step time response(s) of PI controllers.

To attain a fast and simplified control with minimal computation for the estimation of reference currents, I_d* and I_q* are determined using the rated parameters of the induction machine and are derived from the following mathematical expressions:

$$I^*_d = \sqrt{2}\eta_{pu}\frac{kW}{\sqrt{3}V_L\cos\phi}, \text{ and } I^*_q = \sqrt{2}I_{m0} \quad (7)$$

where η_{pu}, kW, and cosΦ denote the efficiency, rated capacity, and full load power factor, respectively. I_{mo} denotes the rms value of the no-load magnetizing current. The predetermined values of I_q* facilitate the action of the controller such that it reaches the exact requirement for the current to attain a fast dynamic compensation of reactive power. The estimated reference currents are reverse transformed and compared with the sensed VSC currents. The error is fed to a hysteresis current controller to force the VSC currents to follow the reference currents and thereby meet the required real and reactive power transaction at the PCC. Such action matches the loading of the IG to the rated value and automatically offsets the fluctuation in the ac-side voltage to yield an ideal rated condition before the generation. The proposed direct current control scheme successfully regulates the voltage and frequency directly through the proper compensation of reactive power and the effective load control across the source. It also facilitates the source's supply of real power to any type of connected load. The control is knitted through three PI controllers, which are tuned such that the power flow across the VSC is regulated to suit the objectives. The PI controller (PI-1) regulating the DC bus acts rapidly to keep the DC bus voltage constant by dumping excess power into the load. By contrast, the slow PI controller (PI-2) used by the VSC to estimate the control component of the I_d current leaves a margin of time that favors the rapid transfer of power across the VSC to enable the system to quickly reach a steady state. The time response against the step input for the deployed PI-1 and PI-2 controllers is depicted in Fig. 5.

The various sections of control are depicted in the comprehensive block diagram of the control scheme (Fig. 4). A fast digital phase locked loop is used to produce the synchronizing signals used by Park and the inverse Park transform. As depicted in Fig. 6, the VSC gating pulses are embedded with the comparator output to protect the PHG

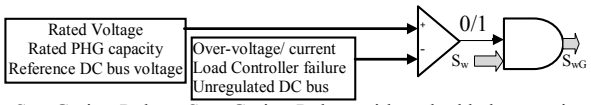

S_w : Gating Pulses, S_{wG}: Gating Pulses with embedded protection

Fig. 6. Protection scheme for fault-immune PHG system.

system from abnormal PCC voltages, source/load currents, and DC bus voltages. In this way, the proposed PHG system becomes immune to faults.

V. Simulation of Proposed Scheme

The proposed control scheme is simulated in MATLAB/Simulink. The machine parameters are maintained at measured values to enable the correct modeling assessment of the control parameters and interface hardware of the actual system (Table I). The model is simulated with the VSC and load controller supporting the IG, which feeds the load emulating that of a BTS. The simulation result indicates the decoupled power control with the VSC to operate with a constant voltage and constant frequency for feeding the load along with the maintenance of the DC bus voltage.

VI. Hardware Implementation

The prototype hardware of the proposed system is developed through the integration of an electrical system with an electronic and power electronic system interfaced with a dS1104 real-time controller, voltage/current sensors, and interfacing circuits. The control scheme is implemented in a laboratory environment for the experimental validation of the simulation results. The parameters of the PHG system are presented in Table I. The V/f-controlled electric drive emulates a pico hydro-based siphon turbine-run system that delivers constant power to the generator. The control scheme is realized through a dS1104 real-time controller that provides switching pulses for the VSC and load controller gating circuits. The controller is run in a closed loop at 12.8 kHz to enable the per cycle collection of 256 samples of different voltages and currents through the voltage and current sensors. The loop is closed at each analog-to-digital converter timer interrupt to sequentially sample the voltage and current values. The choice of 256 samples per cycle enables the easy realization of the moving average filter operating at 100 Hz to facilitate the low-pass filtering of the v_d and v_q voltages, which, when reverse transformed yields the voltage at the PCC. The estimate of I_d current derived from the current of the connected load. A similar moving average filter is also used with samples of the voltage at the DC bus. The hysteresis band switching with 0.1A enables the control of the VSC under the current control mode. The high frequency switching is automatically avoided because of the fixed frequency operation of the real-time controller that prevents the circuit from entering into limit cycles. The PCC

TABLE I
Parameters of the Considered PHG System

System Parameters	
V/f Drive	Delta , e series, 5 kW
Prime Mover	IM, 3-Φ, 3.5 kW, 415 V, 50 Hz., Y, CG
IG	3-Φ, 2.2 kW, 415±10 V, 50 Hz, Y, CG
Filter Cap.	4 µF, 440 V, Y, Epcos
Load	0–2.2 kW at 415±10 V
DC Bus (VSC), V_{DC}*	3,000 µF/1,200 V, 600 V
Line Reactor	6.4 mH, 10 A
Bleeder	600 V, 175 ohm (R)
Control Parameters	*Simulation Parameters*
PI-1(K_p, K_i); 0.09, 0.001	R_s, l_{ls}: 0.035, 0.045
PI-2(K_p, K_i); 0.08, 0.001	R_r',L_{lr}': 0.034, 0.045
PI-3(K_p, K_i); 0.1, 0.01	L_m (pu), J,P: 1.352, 0.0404,2
Hysteresis Band 0.1A	Switching frequency: 12.8 kHz

voltages are sensed through three LEM LV-25P Hall effect voltage sensors. One LEM LV-25PSP5 Hall effect voltage sensor is used to sense the DC bus voltage ranging from 0 V to 800 V. TELCON HTP-25 Hall effect current sensors are used to sense currents in two phases of the VSC. The switching signals are fed to the SKYPER-32 drivers, which provide gate signals to the IGBT module (Semikron GB 128DN) and chopper switch on the DC bus. The test results are recorded using an Agilent DSOX-2014A digital storage oscilloscope and a Fluke 434 power quality analyzer (PQA) to evaluate the steady state and transient state of the system.

VII. Performance Evaluation

Simulation studies are performed on MATLAB/Simulink to evaluate the effectiveness of the proposed scheme. Experimental testing is also conducted to validate the results for the developed prototype hardware. The performance of the proposed system is verified in terms of the following:

1) Steady-state operation of the dual-role VSC
2) Dynamic operation of the dual-role VSC under load perturbations.

A. Simulation Studies

To verify the feasibility of the proposed scheme, MATLAB simulations are performed on the PHG system. The performance of the STATCOM-supported PHGS with intermittent CPL at the PCC is simulated and analyzed through the observed steady-state and dynamic waveforms of the PCC voltage, source currents, STATCOM current, load current, DC bus voltage, etc., as shown in Fig. 7(a–h). The results are analyzed in a three-time duration: (i) t = 2.8 s to 3.0 s: operation of the PHG system during steady state with balanced load at the PCC; (ii) t = 3 s to 3.2 s: load reduction

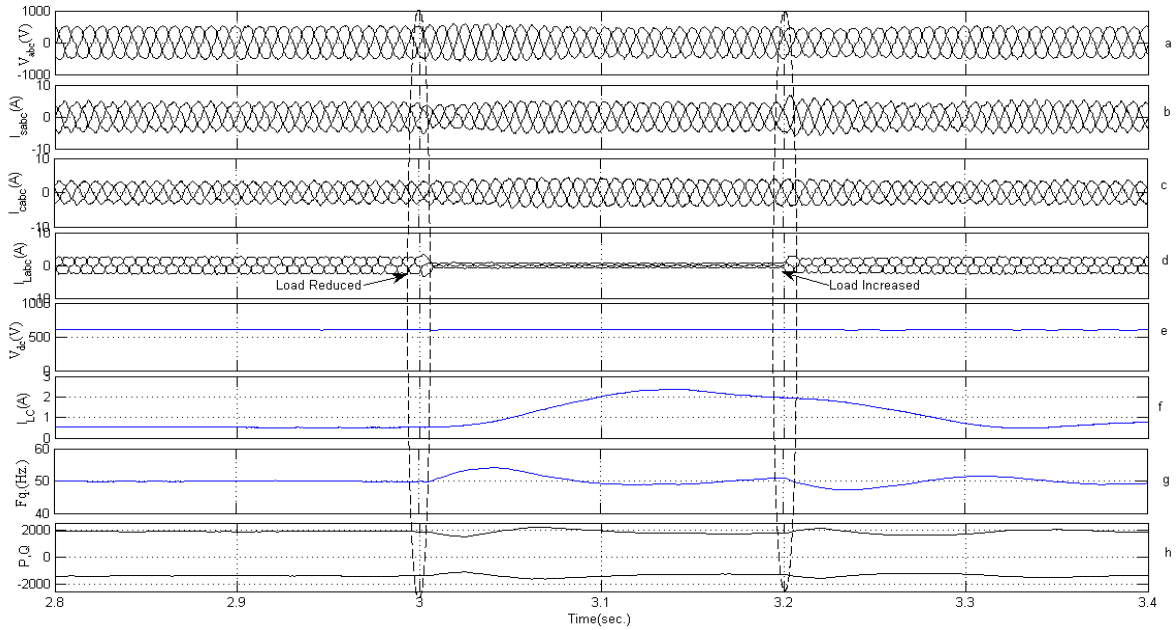

Fig. 7. Simulated performance of CC-VSC supported PHG system feeding loads in the base station of a remote telecom tower. (a) PCC voltage, (b) source current, (c) VSC current, (d) load current, (e) DC bus voltage, (f) source frequency, (g) load controller current, (h) real/ reactive power of source.

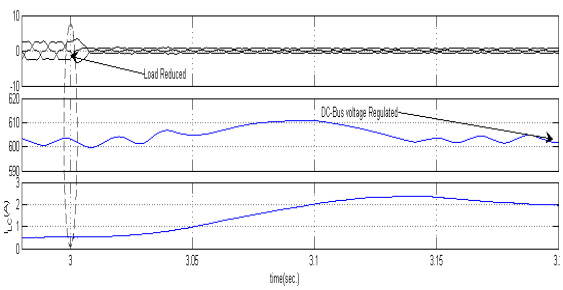

Fig. 8. Dynamics of V_{DC} and current in load controller (i_{LC}).

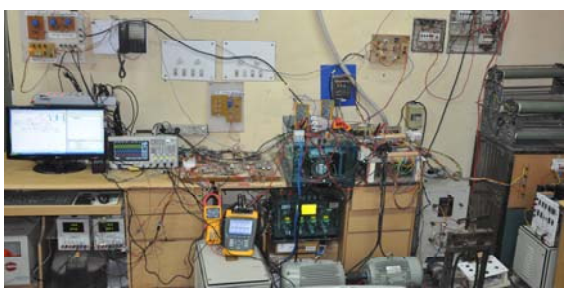

Fig. 9. Prototype experimental setup.

at the PCC; and (iii) t = 3.2 s onward: load reinsertion at the PCC.

As depicted in Fig. 7(a, b) at t = 2.8 s to t = 3 s, the PCC voltage and source currents are regulated and maintained. In this duration, as observed in Fig. 7(c), the VSC supplies the leading current in quadrature with the PCC voltage, presenting it as a VAr generator. Fig. 7(f) depicts the current drawn by the load controller action for the extraction of rated capacity from the PHGS. As observed in Fig. 7(g), the PHGS frequency is well regulated under limits. Fig. 7(e) depicts the regulated DC bus voltage (600 V) that validates the effectiveness of the proposed control scheme during steady-state operation.

The magnified portion of Fig. 7(d–f) portraying the perturbing load current, DC bus voltage, and load controller current is depicted in Fig. 8. At t = 3 s, the load is drastically reduced at the PCC. The light load at the PCC forces the DC voltage to increase at a longer pace with small oscillations because of the delayed response of the PI control corresponding to the load controller and because the excess power starts accumulating in the capacitor at the DC bus of the VSC. However, load controller suitably dumps the excess power, and the current (I_{LC}) starts to increase, which leads to a decrease in the DC bus voltage and prompts the controller to stabilize the DC bus voltage quickly. Therefore, the coordinated action of the controllers for the DC bus regulation and the load controller maintains the DC bus voltage and the constant real power extraction from the source in near steady-state conditions. The performance of the system during intermittent loading at the PCC is explained in the following sections through the experimental results under the same conditions as those in the simulations.

B. Experimental Results

The experimental evaluation of the proposed control scheme is performed using the developed prototype of a 2.2 kW PHG system. The photograph of the experimental setup is shown in Fig. 9. The performance of the PHG system is evaluated experimentally with a current-controlled VSC that feeds a three-phase balanced load in a local distribution grid. The results are depicted in Figs. 10–20. The results are

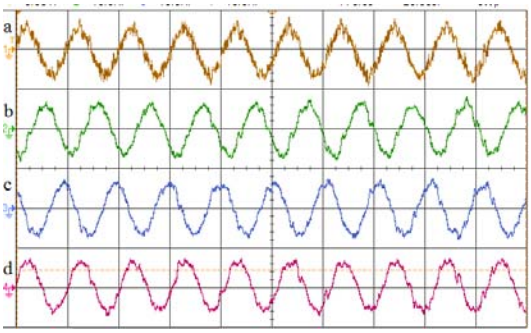

Fig. 10. Oscilloscope traces showing voltage/ph at the PCC of the PHG source currents at steady state. Observed conditions: current, near balanced; voltage and frequency, regulated. [Time scale = 20 ms/div]

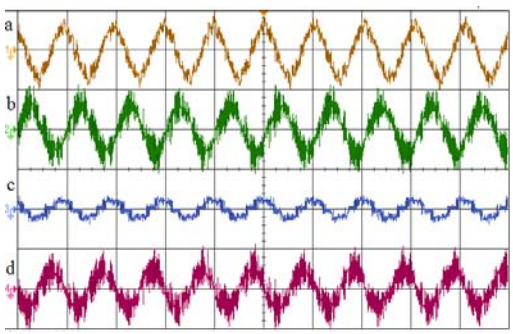

Fig. 11. Oscilloscope traces. (a) PCC voltage/ph. (b) Source current. (c) Load current. (d) STATCOM current at steady state. Observed conditions: source current near in phase opposition (lag), load current in phase, STATCOM current phase quadrature with voltage.

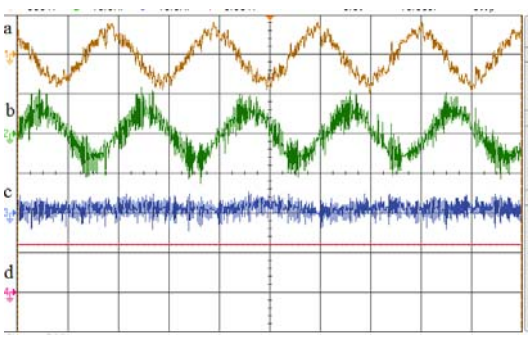

Fig. 12. Oscilloscope traces. (a) PCC voltage. (b) Source current. (c) Current in DC bus. (d) DC bus voltage at steady state. Observed conditions: source current near in phase, deficit source load transferred to load controller via DC bus, DC bus voltage maintained at a set value.

analyzed and depicted through the operation of the dual-role VSC as a STATCOM and load controller to cater to the reactive power requirement of the IG and to provide load matching for remote telecom towers amid the intermittent operation of CPL connected in parallel at the PCC by importing load deviation from the rated condition to the DC bus. In this way, the self-supported DC bus voltage is maintained under rated loading conditions, and load matching by the load controller is achieved through the dissipation of power imported by the VSC on the DC bus.

1) STATCOM Operation under Steady-State CPL: The performance of the STATCOM operation under steady-state conditions with balanced and rated connected load at the PCC is analyzed through the results depicted in Figs. 10–12. A CPL of 0–2 kW and 600 V is connected at the PCC. The oscilloscope traces of the phase voltage and generator source currents are depicted in Fig. 10(a) and Fig. 10(b)–(d), respectively. The PCC voltage and generator source currents are obviously balanced and well regulated. The frequency is also maintained at a rated value upon the rated loading of the IG terminals with 20 ms division of the oscilloscope trace. The voltage and current complete their full cycle in one division.

Fig. 11(a)–(d) depicts the waveform of the PCC phase voltage, source current, load current, and STATCOM current under steady-state conditions. The source current is slightly leading and is nearly opposite the PCC voltage waveform at 180°, thus revealing that the real power is supplied by a generator, which also absorbs negative VAr. The load current is absolutely in-phase, and the STATCOM current is in perfect quadrature and leads with the voltage at the PCC, showing it as a VAr generator. Moreover, applied load is 2.0 kW lower than the IG capacity of 2.2 kW, although this load is effectively equalized through the load controller to maintain constant power withdrawal from the source.

Fig. 12(a)–(d) depicts the source voltage (voltage/ph), source current, load current, and voltage in the DC bus for similar loading conditions. The net power corresponding to the connected load lower than the rated value is absorbed at the DC bus through the VSC by the load controller. The traces shown in Fig. 12(c) also clearly indicate that the current in the DC bus depicts the absorption of power by the load controller. Meanwhile, the DC bus voltage (Fig. 12(d)) is maintained constant at 600 V. The DC bus voltage is self-supported and maintained at a set value throughout the experiment to justify the effectiveness of the proposed scheme.

2) VSC Operation during Intermittent Loading at PCC: The simulation and experimental results depicting load perturbations at the PCC are shown in Figs. (13)–(14) and (15)–(16), respectively. The performance of the PHG system in the simulation under dynamic load perturbations caused by sudden partial load removal and its reinsertion is depicted in Fig. 13(c) at t = 3 and at 3.2 s, respectively. The proposed decoupled control action facilitates load matching and voltage recovery through reactive power compensation. Consequently, as observed in Fig. 13(a), the PCC voltage is regulated throughout the operation. In Fig. 13(b), the current withdrawal from the IG is fixed, and the VSC supplies the requisite leading current in phase quadrature.

The experimental results depicting the performance of the system amid perturbation in load at the PCC are shown in Fig. 15(a)–(d). The three-phase balance load at the PCC (Fig.

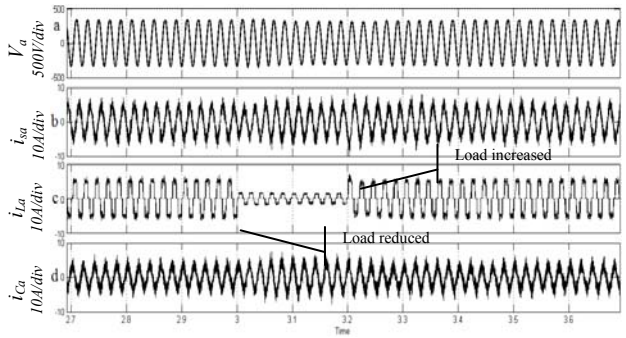

Fig. 13. Simulation results showing the (a) source voltage, (b) source current, (c) load current, and (d) STATCOM current; observed condition: regulated PCC voltage and fixed load perturbation of the source current. rturbing load.

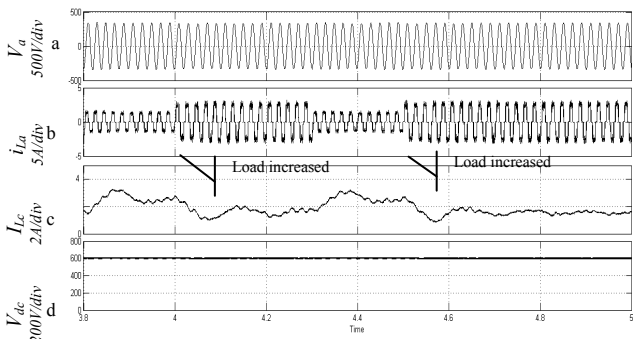

Fig. 14. Simulation results during load perturbations. (a) PCC voltage, (b) load current, (c) load controller current, (d) DC bus voltage. The PCC voltage is maintained at perturbing load, and the deficit/excess load current at the PCC is transferred to the load controller.

15(c)) is reduced after the third division, and the same is increased after the sixth division. Fig. 15(a) shows that the PCC voltage is regulated during load perturbations. In addition, the IG current depicted in Fig. 15(b) is fixed. As shown in Fig. 15(d), the STATCOM supplies the requisite leading current in phase quadrature, thus showing the close match between the experimental and simulation results.

To gain further insights into the action of the load controller and the dissemination of power on the DC bus, we observe the waveform of the current processed by the load controller and the DC bus voltage amid perturbing loads through simulations and experimentations, as presented in Fig. 14(a–d) and Fig. 16(a–d), respectively. The simulation and experimental results show that the DC bus voltage only changes marginally because of the tight control invoked by the load controller. This outcome validates the effective operation of the load controller in realizing load matching for the PHG source. Moreover, the DC bus voltage is well regulated throughout the operation. The test results validate the regulated voltage and frequency at the source terminals and the load matching for the IG under load perturbations, thus justifying the effectiveness of the proposed scheme.

To evaluate further the effectiveness of the proposed scheme for the control of the PHG based low capacity

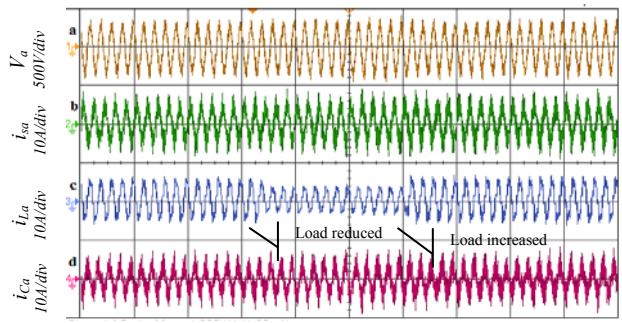

Fig. 15. Experimental results showing the (a) source voltage, (b) source current, (c) load current, and (d) VSC current. Observed condition: the PCC voltage is maintained on perturbing load, and the source current is fixed.

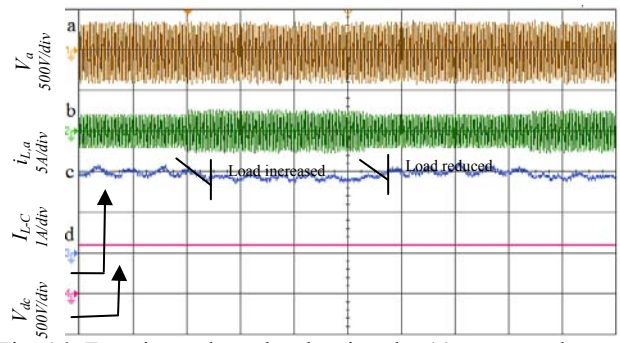

Fig. 16. Experimental results showing the (a) source voltage, (b) load current, (c) DC bus current, and (d) load controller voltage during load perturbations at the PCC. Observed condition: the voltage is regulated, and the DC bus is regulated under dynamic load operations.

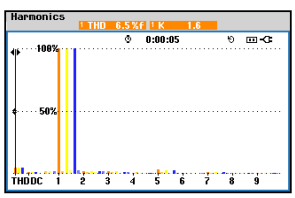

Fig. 17. Harmonic spectrum of PHG source.

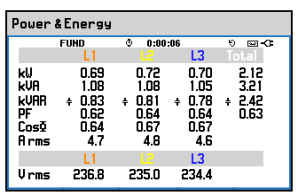

Fig. 18. Power, current, and phase voltage of PHG.

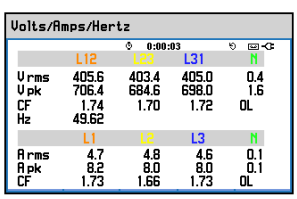

Fig. 19. Screenshots of PQA showing line voltage, frequency, and IG current.

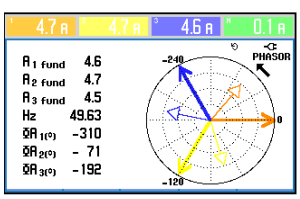

Fig. 20. Voltage and current phasors at source terminals.

pico-hydro system, we use the Fluke 434 PQA for assessing the power quality of the PHG system. The screenshots are shown in Figs. (17)–(20) for the assessment of the generated power by the IG system with support from the STATCOM and load controller. As shown in Fig. 17, the total harmonic distortion of the source current is 6.5%, which is under the acceptable limits for low-capacity generation systems for such applications. The distortion near the switching

frequency can be mitigated easily by employing filters to further improve power quality. Figs. 18–19 show that the IG as a source effectively supplies real power equivalent to its capacity and that STATCOM supplies reactive power for IG magnetization and voltage regulation. The test results obtained with the PQA confirm that the voltage and frequency are well regulated. Fig. 20 depicts the phasor representation of the PCC voltage and PHG source current. The source current, frequency, and phasor are fairly under control and balanced. The system is stable under all limits and caters to the rated capacity loads in continuous duty operation without any overload/overheating.

VIII. CONCLUSIONS

The performance of the PHG system with a self-supported dual-role VSC acting as a STATCOM and load controller is studied through simulation and experimentally validated on a prototype setup. The proposed control scheme effectively regulates the voltage and frequency of the local distribution grid when it caters to intermittent loads in parallel in the base stations of remote telecom towers. As validated with the results, the proposed scheme is effective in meeting the desired conditions. The scheme also ensures that the STATCOM meets the reactive power demand of the system and that the PHG meets the real power demand of the system in a power decoupling manner. The load controller at the DC bus effectively equalizes power flow through the source and maintains constant real power extraction from the source. The proposed control scheme is easy to use and effective, requires a few sensors, and is immune to faults in distribution systems through its embedded auto protection. Moreover, the proposed scheme is effective in generating quality electricity through the pico hydro source for telecom tower applications.

REFERENCES

[1] W. Balshe, "Power system considerations for cell tower applications," in *Proc. Technical Information from Cummins Power Generation*, No. 9019, 2011.

[2] D. Li, W. Saad, I. Guvenc, A. Mehbodniya, and F. Adachi, "Decentralized energy allocation for wireless networks with renewable energy powered base stations," *IEEE Trans. Commun*., Vol. 63, No. 6, pp. 2126-2142, Jun. 2015.

[3] G. M. Dousoky, A. M. El-Sayed, and M. Shoyama, "Improved orientation strategy for energy-efficiency in photovoltaic panels," *Journal of Power Electronics*, Vol. 11, No. 3, pp. 335-341, May 2011.

[4] J. T. Carter, "Siphon pump technology and apparatuses," U.S. Patent 8763625, Jul. 2014.

[5] A. V. Braga, A. J. Rezek, V. F. Silva, A. N. C. Viana, E. C. Bortoni, W. D. C. Sanchez, and P. F. Ribeiro, "Isolated induction generator in a rural Brazilian area: Field performance tests," *Renewable Energy*, Vol. 83, pp. 1352-1361, Nov. 2015.

[6] L. Wang and D. J. Lee, "Coordination control of an AC-to-DC converter and a switched excitation capacitor bank for an autonomous self-excited induction generator in renewable-energy systems," *IEEE Trans. Ind. Appl*., Vol. 50, No. 4, pp. 2828-2836, Jul./Aug. 2014.

[7] B. Singh and V. Rajagopal, "Battery energy storage based voltage and frequency controller for isolated pico hydro systems," *Journal of Power Electronics*, Vol. 9, No. 6, pp. 874-883, Nov. 2009.

Vishal Verma received his B.Tech. degree in Electrical Engineering from the G. B. Pant University of Agriculture and Technology, Pantnagar, India, in 1989, and his M.Tech. and Ph.D. degrees from the Indian Institute of Technology Delhi, New Delhi, India, in 1998 and 2006, respectively. In 1991, he became an Assistant Professor in the Department of Electrical Engineering, G. B. Pant University of Agriculture and Technology, Pantnagar, India, He joined the Delhi Technological University, Delhi, in 2004 as an Associate Professor. He became a full Professor in 2009. He is currently the Dean of Academics in the University. His fields of interest include power electronics, drives, active filters, and power quality issues. Dr. Verma is a member of the Indian Society for Technical Education and a Life Member of the Continuing Education Society of India.

Peeyush Pant received his B.Tech. degree in Electrical Engineering from the Kamla Nehru Institute of Technology, Sultanpur, India, in 1999, and his M.Tech. degree from the Indian Institute of Technology Delhi, New Delhi, India, in 2005. He is currently a Research Scholar in the Department of Electrical Engineering, Delhi Technological University, Delhi, India. His research interests include renewable energy, power electronics, electric machinees, and drives.

Bhim Singh received his B.E. (Electrical) degree from the University of Roorkee, Roorkee, India, in 1977, and his M.Tech. (Power Apparatus and Systems) and Ph.D. degrees from the Indian Institute of Technology (IIT) Delhi, New Delhi, India, in 1979 and 1983, respectively. In 1983, he joined the Department of Electrical Engineering, University of Roorkee as a Lecturer. He became a Reader in 1988. In December 1990, he joined the Department of Electrical Engineering, IIT Delhi, as an Assistant Professor and became an Associate Professor in 1994 and a Professor in 1997. He has guided 59 Ph.D. dissertations and 156 M.E./M.Tech. thesis. He has been granted 1 U.S. patent and has filed 17 Indian patents. He has executed more than 75 sponsored and consultancy projects. Prof. Singh is a Fellow of the Indian National Academy of Engineering, the National Science Academy, the Indian Academy of Science, the Institute of Engineering and Technology U.K., the Institution of Engineers (India), the World Academy of Sciences (FTWAS), the Indian National Science Academy, and the Institution of Electronics and Telecommunication Engineers. He also received the Shri Om Prakash Bhasin Award in 2014 for his work in the field of engineering, including energy and aerospace.